Articles

Encapsulation of Gold Nanoclusters in Silica Materials via an Inverse Micelle/Sol−Gel Synthesis

Anthony Martino,*,† Stacey A. Yamanaka,‡ Jeffrey S. Kawola,† and Douglas A. Loy§

Fuel Science Department, Sandia National Laboratories, Albuquerque, New Mexico 87185-0710; Texas Instruments, Mail Station 147, P.O. Box 655936, Dallas, Texas 75265; and Properties of Organic Materials Department, Sandia National Laboratories, Albuquerque, New Mexico 87185-1407

Received September 4, 1996. Revised Manuscript Received November 12, 1996⊗

Nanometer-sized gold particles were encapsulated in the micropores of xerogels and aerogels. The synthesis involves the sequential reduction of a gold salt followed by sol−gel processing in an inverse micelle solution. The inverse micelle solution solubilizes the metal salt and provides a microreactor for the nucleation, growth, and stabilization of the nanometer-sized clusters. Hydrolysis and condensation of an added siloxane precursor produces a wet gel embedding the particles. Characterization of the particle size and composition and the particle growth process was completed with transmission electron microscopy (TEM), electron diffraction, and UV−visible absorption spectrometry. Characterization of the gel surface areas was completed with N_2 porosimetry. Material properties determined as a function of the gel precursor (TEOS vs a prehydrolyzed form of TEOS), the water to gel precursor reaction stoichiometry, and surfactant concentration are discussed in terms of the unique solution chemistry occurring in the microheterogeneous inverse micelle solutions.

Introduction

Colloidal-sized metal and semiconductor particles with diameters of 1−20 nm (nanoclusters) are of current interest because they mark a material transition range between molecular and bulk properties. With decreasing colloid size, bulk properties are lost as the continuum of electronic states breaks down (i.e., quantum size effects) and as the fraction of surface atoms becomes large. There are a number of ways to synthesize metal particles with diameters between 1 and 20 nm.[1−3] All synthesis routes include nucleation, growth, and stabilization of the particles and attempt to control particle size, size distribution, chemical composition, and structure. Chemical or photolytic reduction,[4−6] thermal decomposition,[7−9] and vapor phase condensation[10−12] of metal salts and organometallic reagents initiates nucleation and growth. Controlling double-layer forces with buffers and electrolytes[13,14] and the use of steric stabilizing agents such as polymers,[15−24] surfactants,[25−34] and bulky ligand appendages[35−42] stabilize the particles in solution.

* To whom correspondence should be addressed (martino@sandia.gov).
† Fuel Science Department, Sandia National Laboratories.
‡ Texas Instruments.
§ Properties of Organic Materials Department, Sandia National Laboratories.
⊗ Abstract published in *Advance ACS Abstracts,* January 1, 1997.

(1) Bradley, J. S. *Clusters and Colloids, From Theory to Applications*; Schmid, G., Ed.; VCH Publications, Inc.: New York, 1994; Chapter 6.
(2) Steigerwald, M. L.; Brus, L. E. *Annu. Rev. Mater. Sci.* **1989**, *19*, 471.
(3) Henglein, A. *Chem. Rev. (Washington, D.C.)* **1989**, *89*, 1861.
(4) Shen, J.; Hu, Z.; Hsia, Y.; Chen, Y. *Appl. Phys. Lett.* **1991**, *59*, 2510.
(5) Takiyama, K. *Bull. Chem. Soc. Jpn.* **1958**, *31*, 944.
(6) Turkevich, J.; Stevenson, P. C.; Hillier, J. *J. Chem. Soc., Faraday Discuss.* **1951**, *11*, 55.
(7) Brennan, J. G.; Siegrist, T.; Carroll, P. J.; Stuczynski, S. M.; Brus, L. E.; Steigerwald, M. L. *J. Am. Chem. Soc.* **1989**, *111*, 4141.
(8) Hoon, S. R.; Kilner, M.; Russell, G. J.; Tanner, B. K. *J. Magn. Magn. Mater.* **1983**, *39*, 107.
(9) Griffiths, C. H.; O'Horo, M. P.; Smith, T. W. *J. Appl. Phys.* **1979**, *50*, 7108.
(10) Lin, S. T.; Franklin, M. T.; Klabunde, K. J. *Langmuir* **1986**, *2*, 259.
(11) Kimura, K.; Bandow, S. *Bull. Chem. Soc. Jpn.* **1983**, *56*, 3578.
(12) Francis, C. G.; Huber, H.; Ozin, G. A. *Inorg. Chem.* **1980**, *19*, 219.
(13) Quinn, M.; Mills, G. *J. Phys. Chem.* **1994**, *98*, 9840.
(14) Trivino, G. L.; Klabunde, K. J.; Dale, E. B. *Langmuir* **1987**, *3*, 986.
(15) Ng Cheong Chan, Y.; Schrock, R. R.; Cohen, R. E. *Chem. Mater.* **1992**, *4*, 24.
(16) Cummins, C. C.; Schrock, R. R.; Cohen, R. E. *Chem. Mater.* **1992**, *4*, 27.
(17) Ishizuki, N.; Torigoe, K.; Esumi, K.; Meguro, K. *Colloids Surf.* **1991**, *55*, 15.
(18) Mahler, W. *Inorg. Chem.* **1988**, *27*, 435.
(19) Wang, Y.; Suna, A.; Mahler, W.; Rasowski, R. J. *J. Chem. Phys.* **1987**, *87*, 7315.
(20) Kuczynski, J. P.; Milosavljevic, B. M.; Thomas, J. K. *J. Phys. Chem.* **1984**, *88*, 980.
(21) Mau, A. W. H.; Huang, C. B.; Kakuta, N.; Bard, A. J.; Campion, A.; White, M. J.; Webber, S. E. *J. Am. Chem. Soc.* **1984**, *106*, 6537.
(22) Fojtik, A.; Weller, H.; Koch, U.; Henglein, A. *Ber. Bunsen-Ges. Phys. Chem.* **1984**, *88*, 969.
(23) Meisssner, D.; Memming, D.; Kastening, B. *Chem. Phys. Lett.* **1983**, *96*, 34.
(24) Hess, P. H.; Parker, P. H. *J. Appl. Polym Sci.* **1966**, *10*, 1915.
(25) Torigoe, K.; Esumi, K. *Langmuir* **1992**, *8*, 59.
(26) Esumi, K.; Shiratori, M.; Ishizuka, H.; Tano, T.; Torigoe, K.; Meguro, K. *Langmuir* **1991**, *7*, 457.
(27) Zhao, X. K.; Xu, S.; Fendler, J. H. *Langmuir* **1991**, *7*, 520.

S0897-4756(96)00462-0 CCC: $14.00

A common nanocluster synthesis technique is the reduction of metal salts in inverse micelle solutions.[25−34] Inverse micelles are solution structures formed by the self-assembly of surfactants in apolar solvents (i.e., toluene, alkanes). Surfactants possess two distinct moieties, a hydrophilic headgroup and a hydrophobic tail group, and they self-assemble in apolar solvents so that the hydrophilic headgroups shield themselves from the oleic surroundings.[43] The relatively polar headgroup regions solubilize and confine added metal salts and act as reaction cages when a reducing agent is introduced. Ultrasmall, monodispersed particles sterically stabilized in solution by surfactant are formed. Advantages of the inverse micelle synthesis technique include mean particle size control and compositional variety. Particle size control results from regulation of the nucleation site size (inverse micelle size) and the particle growth rate (material exchange rate between inverse micelles). A variety of metals and bimetallics are produced by choosing different metals salts and mixtures of metal salts. Unfortunately, the presence of surfactant hinders potential applications (i.e., catalysis), and removal of the surfactant causes immediate flocculation of the particles with loss of the unique and interesting material properties.

Our goal is to isolate nanoclusters and preserve their unique properties without the presence of any stabilizing agents that attach themselves to the particle surface. We have developed sol−gel processing in inverse micelle, nanocluster solutions to encapsulate or sterically entrap nanoclusters in the micropores of xerogels and aerogels. The synthesis is a sequential reduction of a metal salt and sol−gel processing of an added siloxane precursor in an inverse micelle solution. Sol−gel processing of porous silica gels in polar solvents has been used to encapsulate a variety of large molecules including laser dyes, photochromics, and proteins.[44−50] Sol−gel encapsulation involves polymerization of a gel precursor, usually tetramethoxysilane or tetraethoxysilane, to build the silica gel structure (host) around the dopant (guest). Steric entrapment occurs when the gel pore size is comparable to the dopant size. Also, nanometer-sized gold particles have been stabilized with a silica coating using silane coupling agents as surface primers.[51] The product of this work includes nanoclusters in a silica monolith that remain small, of one size, and highly dispersed even after the removal of the surfactant.

Other works involving sol−gel processing in surfactant, apolar solvent solutions use high surfactant or alcohol concentrations and are not suitable for monodisperse cluster formation.[52−58] We have established an entirely new system with low surfactant concentrations and no alcohol. The inverse micelle solutions and precursor salt solutions are characterized by small-angle X-ray scattering (SAXS). After chemical reduction of the metal salt and hydrolysis and condensation of an added siloxane precursor, cluster size, chemical composition, and the cluster growth process are characterized by transmission electron microscopy (TEM), electron diffraction, and UV−visible absorption spectrometry. Gel surface areas are determined by N_2 porosimetry. Material properties are determined as a function of the gel precursor (TEOS vs the prehydrolyzed form of TEOS), the water to gel precursor reaction stoichiometry (molar ratio = 4:1, 3:1, 2:1, and 1:1), surfactant concentration, drying mechanism, and process washing with hexanol.

We are currently interested in nanocluster-gel materials as catalysts. Metal−gel matrixed materials have been extensively studied as catalysts, because high surface area, high porosity gels act to disperse the active metal, minimize mass transfer and pore diffusion limitations, and promote activity through tunable surface acidities. Traditionally, atomic metals are added to gels when salts are ion-exchanged with terminal hydroxyl groups on the gel,[59,60] through impregnation into the gel backbone during gel processing,[61−64] or through the use of chelating agents.[65,66] Clusters are formed later through chemical, thermal, and photolytic reduction. No current synthesis method prevents metal particle sin-

(28) O'Sullivan, E. C.; Patel, R. C.; Ward, A. J. I *J. Colloid Interface Sci.* **1991**, *146*, 582.
(29) Larpent, C.; Brisse-Le Menn, F.; Patin, H. *J. Mol. Catal.* **1991**, *65*, L35.
(30) Borgarello, E.; Lawless, D.; Serpone, N.; Pelizzetti, E.; Meisel, D. *J. Phys. Chem.* **1990**, *94*, 5048.
(31) Maguro, K.; Torizuka, M.; Esumi, K. *Bull. Chem. Soc. Jpn.* **1988**, *61*, 341.
(32) Monserrat, K.; Gratzel, M.; Tundo, P. *J. Am. Chem. Soc.* **1980**, *102*, 5527.
(33) Kiwi, J.; Gratzel, M. *J. Am. Chem. Soc.* **1979**, *101*, 721.
(34) Chen, J. P.; Sorensen, C. M.; Klabunde, K. J. *Phys. Rev. B* **1995**, *51*, 11527.
(35) Nosaka, Y.; Ohta, N.; Fukuyama, T.; Fujii, N. *J. Colloid Interface Sci.* **1993**, *155*, 23.
(36) Duan, Z.; Hampden-Smith, M. J.; Datye, A.; Nigrey, P.; Quintana, C.; Sylwester, A. P. *J. Catal.* **1993**, *139*, 504.
(37) Folkers, J. P.; Laibinis, P. E.; Whitesides, G. M. *Langmuir* **1992**, *8*, 1330.
(38) Zimmermann, F.; Wokann, A. *Mol. Phys.* **1991**, *73*, 959.
(39) Becker, C.; Fries, T., Wendelt, K.; Kreibig, U.; Schmid, G. *J. Vac. Sci. Technol. B* **1991**, *9*, 810.
(40) Hayes, D.; Meisel, D.; Micic, O. I. *Collods Surf.* **1990**, *55*, 121.
(41) Andrews, M. P.; Ozin, G. A. *J. Phys. Chem.* **1986**, *90*, 2929.
(42) Henglein, A. *J. Phys. Chem.* **1979**, *83*, 2209.
(43) Langevin, D. *Acc. Chem. Res.* **1988**, *21*, 255.
(44) Zusman, R.; Rottman, C.; Ottolenghi, M.; Avnir, D. *J. Non-Cryst. Solids* **1990**, *122*, 107.
(45) Braun, S.; Rappoport, S.; Zusman, R.; Avnir, D.; Ottolenghi, M. *Mater. Lett.* **1990**, *10*, 1.
(46) Dunn, B.; Zink, J. I. *J. Mater. Chem.* **1991**, *1*, 903.
(47) Yamanaka, S. A.; Nishida, F.; Ellerby, L. M.; Nishida, C. R.; Dunn, B.; Valentine, J. S.; Zink, J. I *Chem. Mater.* **1992**, *4*, 495.
(48) Ellerby, L. M.; Nishida, C. R.; Nishida, F.; Yamanaka, S. A.; Dunn, B.; Selverstone Valentine, J.; Zink, J. I. *Science* **1992**, *255*, 1113.
(49) Avnir, D.; Braun, S.; Ottolenghi, M. *Supramolecular Architecture*; 1992; Chapter 27.
(50) Wu, S.; Ellerby, L. M.; Cohan, J. S.; Dunn, B.; El-Sayed, M. A.; Selverstone Valentine, J.; Zink, J. I. *Chem. Mater.* **1993**, *5*, 115.
(51) Liz-Marzan, L. M.; Giersig, M.; Mulvaney, P. *Langmuir* **1996**, *12*, 4329.
(52) Guizard, C.; Larbot, A.; Cot, L.; Perez, S.; Rouviere, J. *J. Chim Phys.* **1990**, *87*, 1901.
(53) Guizard, C.; Stitou, M.; Larbot, A.; Cot, L.; Rouviere, J. *Mater. Res. Soc. Symp. Proc.* **1988**, *121*, 115.
(54) Murakata, T.; Sato, S., Ohgawara, T.; Watanabe, T.; Suzuki, T. *J. Mater. Sci.* **1992**, *27*, 1567.
(55) Friberg, S. E.; Yang, C. C.; Sjoblom, J. *Langmuir* **1992**, *8*, 372.
(56) Friberg, S. E.; Yang, C. C. *Innovations in Materials Processing Using Aqueous Colloid and Surface Chemistry*; Doyle, F. M.; Raghavan, S.; Somasundaran, P.; Warren, G. W., Eds.; The Minerals, Metals, & Materials Society, 1988; p 181.
(57) Jones, S. M.; Amran, A.; Friberg, S. E. *J. Disp. Sci. Technol.* **1994**, *15*, 513.
(58) Lessard, R. B.; Wallace, M. M.; Oertling, W. A.; Chang, C. K.; Berglund, K. A.; Nocera, D. G. *Mater. Res. Soc. Symp. Proc.* **1989**, *155*, 109.
(59) Tominaga, H.; Ono, Y.; Keii, T. *J. Catal.* **1975**, *40*, 197.
(60) Ikoma, S.; Takano, S.; Nomoto, E.; Yokoi, H. *J. Non-Cryst. Solids* **1989**, *113*, 130.
(61) Morke, W.; Lamber, R.; Schubert, U.; Breitscheidel, B. *Chem. Mater.* **1994**, *6*, 1659.
(62) Ishiyama, J. I.; Kurokawa, Y.; Nakayama, T.; Imaizumi, S.; *Appl. Catal.* **1988**, *40*, 139.
(63) Lopez, T.; Villa, M.; Gomez, R. *J. Phys. Chem.* **1991**, *95*, 1690.
(64) Lopez, T.; Lopez-Gaona, A.; Gomez, R. *Langmuir* **1990**, *6*, 1343.
(65) Moon Choi, K.; Shea, K. J. *J. Am. Chem. Soc.* **1994**, *116*, 9052.
(66) Hardee, J. R.; Tunney, S. E.; Frye, J.; Stille, J. K. *J. Polym. Sci., Part A: Polym. Chem.* **1990**, *28*, 3669.

tering under robust catalytic conditions, however. Our work is the first where formation of clusters proceeds formation of the gel, thus resulting in encapsulation and potentially new advantages. Clusters are trapped in the gel pores of comparable size limiting the modes of particle sintering. The advantages of the inverse micelle technique are retained including formation of ultrasmall, monodisperse, highly dispersed particles, and particle size and composition control (i.e., various metals, mixtures of different metals, alloys, layered particles, metal oxides, and metal sulfides).

Experimental Section

Materials. The surfactant didodecyldimethylammonium bromide (DDAB), apolar solvent toluene (99.9+% purity), reducing agent lithium borohydride in tetrahydrofuran (2 M), gold trichloride, tetraethyl orthosilicate (TEOS), and a 40 wt % tetrabutylammonium hydroxide (TBAOH) in water solution were purchased from Aldrich and used as delivered. Poly(diethoxysiloxane) (MW = 610 g/mol), an oligomer of TEOS formed by a proprietary prehydrolysis reaction, was purchased from United Chemical Technologies of Bristol, PA, and used as delivered. Hexanol is used as a washing solvent and is purchased from Aldrich at 99.9+% purity.

Synthesis. Surfactant is added to toluene (1−5 wt %) and stirred by hand shaking to form the inverse micelle solution. $AuCl_3$ (0.001 M) and the gel precursor (0.4 M) are added, and the solution is stirred until the salt is fully solubilized. A gold colored transparent solution is formed. The $LiBH_4$/THF solution is injected into the salt precursor solution under rapid stirring so that the $[BH_4^-]$:$[Au^{3+}]$ = 3:1. The gold solution immediately turns dark purple. The 40 wt % TBAOH in water solution is added 1−5 min afterward, and the gelation time is marked when the solution no longer flows under gravity. A deep purple, viscous gel is formed. The water-to-gel precursor molar ratio is studied as an experimental variable and is set at 1:1, 2:1, 3:1, and 4:1. Two different gel precursors are tested: TEOS and a prehydrolyzed form of TEOS. The gels are aged for 14 days prior to drying under ambient conditions to form xerogels or under supercritical CO_2 extraction to form aerogels. Some samples were washed to remove surfactant and reaction byproducts by passing warm hexanol over the dried, crushed gels through an aspirator funnel. Samples discussed in the Results were not washed unless indicated.

Characterization. SAXS was completed at the Small-Angle Scattering Center at the University of New Mexico. A 12 kW rotating anode source was used with a Kratky camera and an M-Braun linear position-sensitive detector. A Ni filter was used as a monochromator, and the samples were sealed in quartz capillary tubes. Particle size and composition in the colloidal solutions were characterized with transmission electron microscopy (TEM) and electron diffraction. These tests were performed with a 300 keV Phillips CM30 electron microscope. Dried, crushed gels were dispersed over a holey carbon substrate. UV−visible absorption spectroscopy was completed with a Hewlett-Packard 8452A diode array spectrophotometer. Quartz cuvettes were used in liquid samples, and gels were sliced and mounted on quartz microscope slides. BET surface area analysis of the crushed xerogels and aerogels was carried out with a Quantachrome Autosorb-6 surface analysis apparatus.

Results

Small-angle X-ray scattering was used to characterize the inverse micelle solutions and the effect of the addition of the gold salt and gel precursors to the solution structure. SAXS of DDAB/toluene inverse micelle solutions, gold salt in DDAB/toluene inverse micelle solutions, and gold salt and TEOS in DDAB/toluene inverse micelle solutions is weak but existent. Scattering curves are flat and bend only at relatively large scattering angles. Guinier analysis indicates the

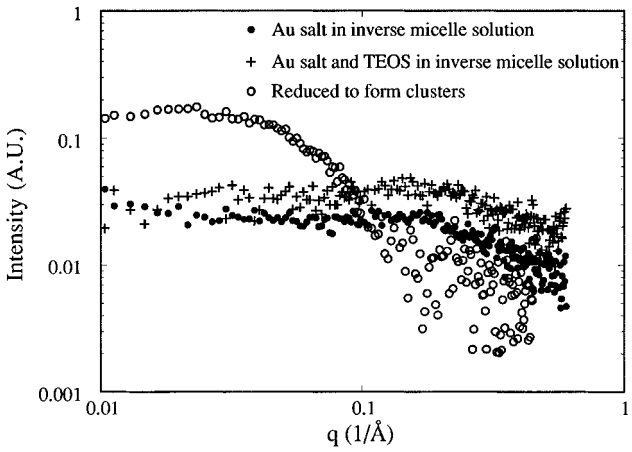

Figure 1. Small-angle X-ray scattering of DDAB/toluene inverse micelles with (a) added Au salt, (b) added Au salt and TEOS, (c) Au clusters in the presence of TEOS. No SAXS is observed when only TEOS is added to DDAB/toluene. The precursor solutions show small aggregate structures (R_g = 0.49 nm). The cluster size as detected by SAXS (R_g = 2.34 nm) is slightly smaller than when measured by TEM. $q = (4\pi/\lambda)$ sin θ where λ is the wavelength of the radiation and 2θ is the scattering angle.

aggregate size, R_g = 0.49 nm, remains constant in all three cases (Figure 1). No small-angle X-ray scattering is observed when only TEOS is added to DDAB/toluene mixtures. Finally, scattering and Guinier analysis of gold salt and TEOS solutions after reduction (i.e., after cluster formation, but before hydrolysis and condensation) indicates a cluster size of R_g = 2.34 nm.

Formation of the clusters occurs within seconds after addition of the reducing agent. The gold solutions turn purple, the color indicative of the presence of colloidal sized gold. Gelation occurs in the cluster, surfactant solutions at 1.5, 2.5, 3.3, and 24 h after the addition of TBAOH/H_2O for samples with the reaction stoichiometry of 1:1, 2:1, 3:1, and 4:1 molar ratio of water to TEOS. The prehydrolyzed TEOS precursor samples gel much more quickly compared to the TEOS precursor. With the molar ratio of water to TEOS oligomer = 4:1, gelation occurs in 15 min. For reaction stoichiometries of 3:1 and less, gelation occurs within 5 min. The basic water solution is fully solubilized in the inverse micelle solution before gelation. The clusters are embedded in the gels upon gelation. The solutions are transparent and clear (yet colored) at all water concentrations, and no cloudiness or indication of phase separation is visibly apparent.

All wet gels are transparent, homogeneously deep purple, viscous, and undergo little to no synerises (Figure 2). Drying to form xerogels causes the gels to shrink $^1/_3$ to $^1/_2$ of their original volume independent of reaction stoichiometry and precursor type. Deep purple monoliths are formed. Drying to form aerogels causes little shrinking in prehydrolyzed TEOS gels and shrinks TEOS precursor gels by $^1/_2$ of their original volume. Aerogels appear chalky and light purple but regain their color when wetted.

The synthesis produces highly dispersed, monodispersed, nanometer-sized gold particles embedded in silica matrixes (Figure 3). Particle size is tested as a function of reaction stoichiometry, the gel precursor type, the drying procedure, and washed vs unwashed samples. Particle size is independent of reaction stoichiometry, gel precursor type, and the effect of washing

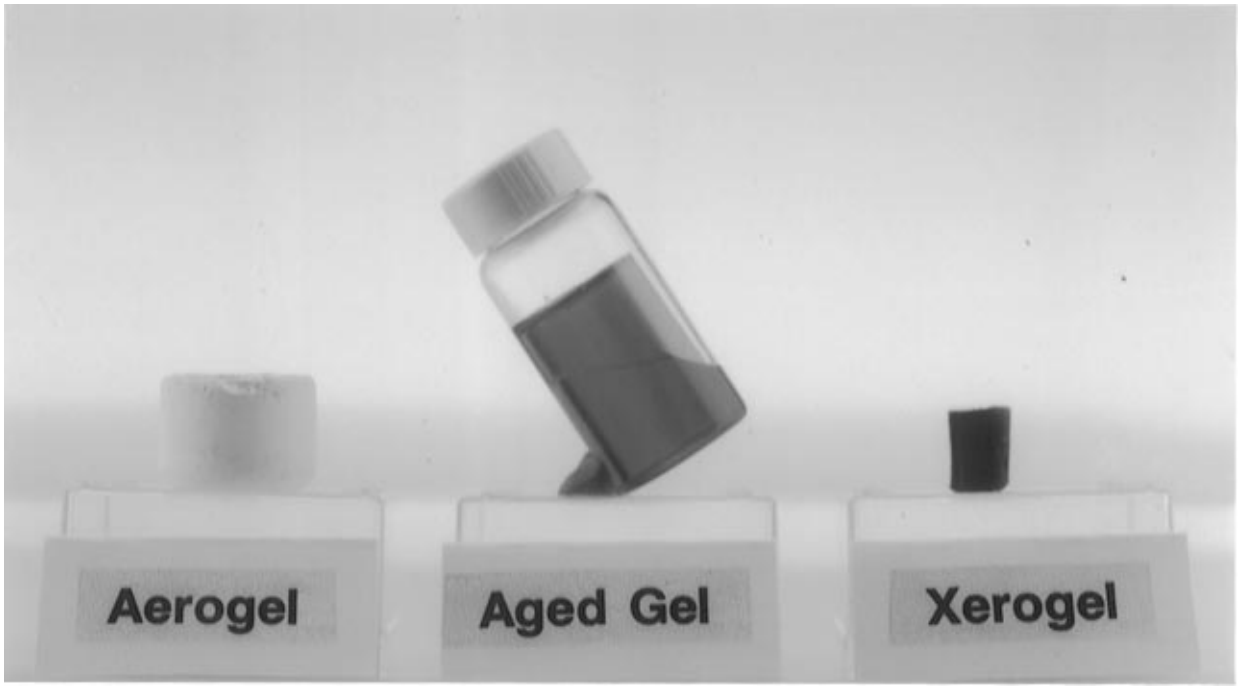

Figure 2. Picture of typical wet gels, xerogels, and aerogels with sterically entrapped Au clusters. Aged gels and xerogels retain the purple color of colloidal Au. Aerogels lose most color, but become purple when rewet with toluene.

Figure 3. TEM of Au clusters embedded in silica matrix. The particles are 5.7 nm in diameter and highly dispersed. Particle size is roughly twice that of Au clusters synthesized in tradiational DDAB/toluene solutions without TEOS. Particle size is independent of gel precursor type, drying procedure, or the H_2O:Si ratio.

(Table 1). The size distribution of a typical sample is relatively narrow (Figure 4). For washed samples, particle size is independent of the drying procedure (xerogels vs aerogels). It appears that the particles are washed out of samples made with the prehydrolyzed form of the TEOS precursor. Few are observed within

Table 1. Particle Diameters in Nanometers as a Function of Reaction Stoichiometry, Drying Process, Precursor Type, and Hexanol Washing

	aerogels				xerogels			
	TEOS		prehydrolyzed TEOS		TEOS		prehydrolyzed TEOS	
H_2O:Si	washed	not washed	washed	not washed	washed	not washed	washed	not washed
2:1	5.8 ± 1.3	5.6 ± 1.5	5.7 ± 1.3	N/A	N/A	6.0 ± 1.5	N/A	N/A
4:1	5.6 ± 1.1	6.7 ± 1.1	N/A	N/A	N/A	6.7 ± 2.2	N/A	7.1 ± 1.2

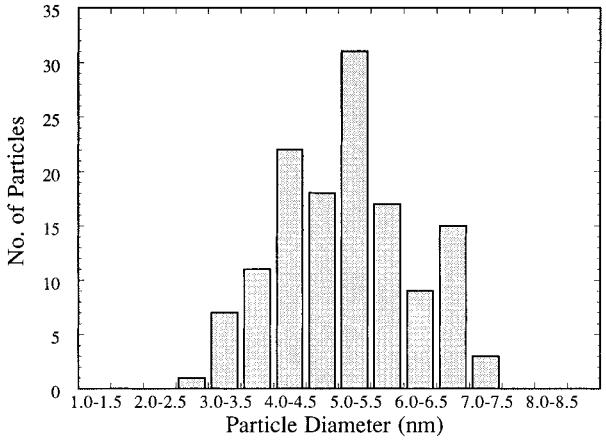

Figure 4. Size distribution as determined by TEM indicating average particle size and monodispersity.

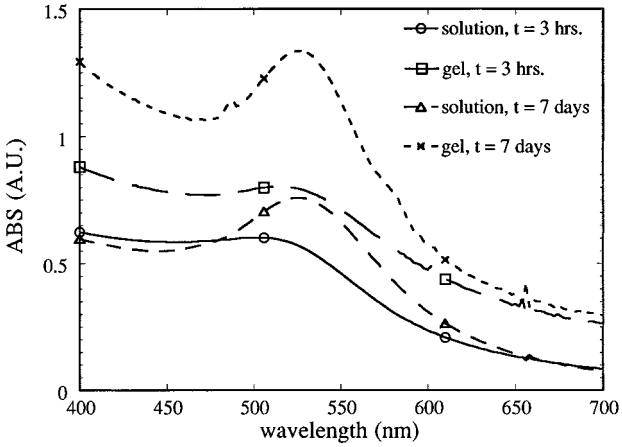

Figure 5. UV−visible spectrum of Au cluster as a function of time and gelled and ungelled samples. The plasmon resonance red shifts with time as the particles grow. The growth rate is faster in gelled samples, but final particle size is independent of the gelation process.

the gel by TEM. Particle size is roughly twice as large in gels as in pure inverse micelle solutions of DDAB and toluene.[67] Electron diffraction from the clusters show five rings that index to the presence of FCC−Au. The relative diffraction peak radii for the five rings are 1.0, 0.86, 0.61, 0.52, and 0.40. It should be noted that our work with Pd systems indicate 0.01 M metal salt precursor solutions result in approximately 1 wt % Pd on SiO_2 materials as measured by atomic adsorption spectroscopy.

Monitoring cluster size in solution and in wet gels as a function of time provides information on the growth mechanism and the effect of gelation on particle growth. Size is monitored by measuring the gold plasmon resonance observed by UV−visible spectroscopy. Colloidal sized gold in solution exhibits a plasmon resonance between 500 and 550 nm depending on particle size. Increasing particle size results in a red-shift in the plasmon resonance. Immediately after salt reduction, the gold plasmon resonance occurs at 502 nm in gel precursor, DDAB, and toluene solutions. The plasmon resonance red-shifts to 509 nm after 3 h and stabilizes at 526 nm after 7 days (Figure 5). If gelation is initiated to a new sample by adding TBAOH/water to the solution, the gold plasmon resonance is 518 and 527 nm after 3 h and after 7 days, respectively (Figure 5). The particles slowly grow after the reduction before stabilizing in both ungelled and gelled samples. The particle growth mechanism is faster, but the final particle size is unaffected by the gelation process (assuming constant medium refractive indexes between ungelled and gelled samples).

Surface areas as determined by N_2 porosimetry are strongly dependent on the reaction stoichiometry, surfactant concentration, and gel precursor type. With some exceptions, aerogel surface areas increase as the molar ratio of water-to-gel precursor increases and as surfactant concentration decreases (Figures 6 and 7). Aerogels formed with prehydrolyzed TEOS precursor exhibit higher surface areas than when formed with TEOS (compare Figures 6a and 7a). When gold is embedded in the silica matrixes, the surface areas increase and follow the same trend with reaction stoichiometry (Figures 6b and 7b). To determine if the surfactant changes the reaction chemistry and thus the material properties or obstructs the silica surface, the materials were washed with warm hexanol. Surface areas increase and follow similar trends with reaction stoichiometry (Figures 6b and 7b). TEOS xerogels exhibit negligible surface areas (not shown). Prehydrolyzed TEOS xerogels (not shown) exhibit similar surface areas and trends as do prehydrolyzed TEOS aerogels (Figure 7a). The silica matrixes are mesoporous with pore diameters ranging from 5 to 30 nm.

Discussion

SAXS indicates that inverse micelles formed in DDAB/toluene solutions are small (R_g = 0.49 nm) with only a few surfactant molecules forming each aggregate structure. SAXS also indicates that the addition of gold salt or the addition of both gold salt and TEOS have no effect on aggregate size. However, SAXS is not observed when only TEOS is added to inverse micelle solutions. TEOS alone causes dissolution of the surfactant aggregate structures. TEOS is miscible in toluene, but relatively polar. The driving force for surfactant aggregation decreases as the gel precursor acts as a cosolvent for toluene and the polar moieties of the surfactant. It is likely that there is some effect of TEOS on gold salt inverse micelle structures, and the effect is offset by the salt or not detected due to weak scattering.

The size of particles formed by the reduction of metal salts in typical inverse micelle solutions depends on the inherent size of the inverse micelles and the material exchange rate between inverse micelles. Both micelle

(67) Wilcoxon, J. P.; Williamson, R. L.; Baughman, R. *J. Chem. Phys.* **1993**, *98*, 9933.

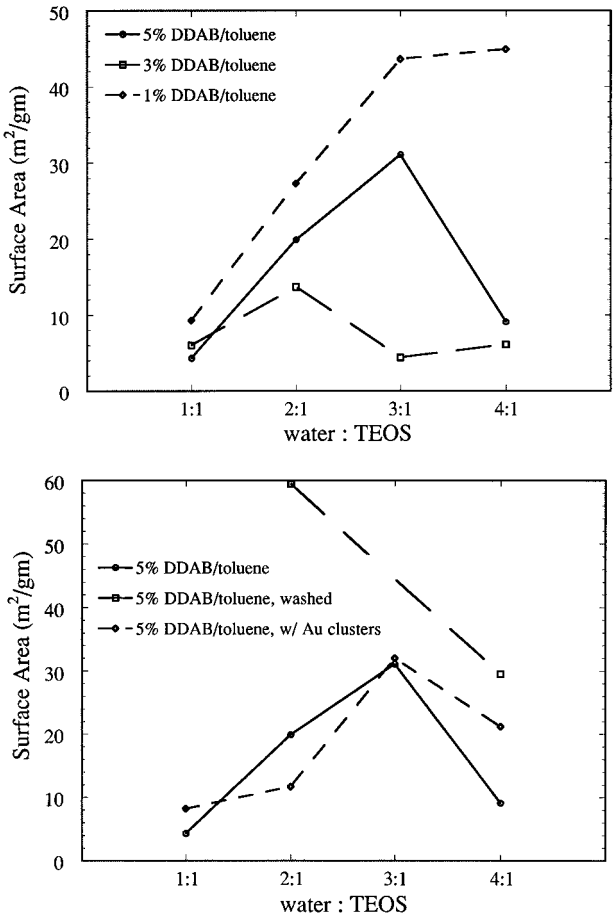

Figure 6. (a, top) BET surface areas of TEOS aerogels as a function of the H_2O:Si ratio and surfactant concentration. Au salt or clusters are not present. The materials are mesoporous. Surface areas generally increase with the reaction stoichiometry and decreasing surfactant concentration. BET surface areas of TEOS xerogels are negligible. (b, bottom) BET surface areas of TEOS aerogels as a function of hexanol washing and cluster presence. Surface area's increase when surfactant is washed from the pores. The presence of Au salt or clusters has no effect of gel surface areas.

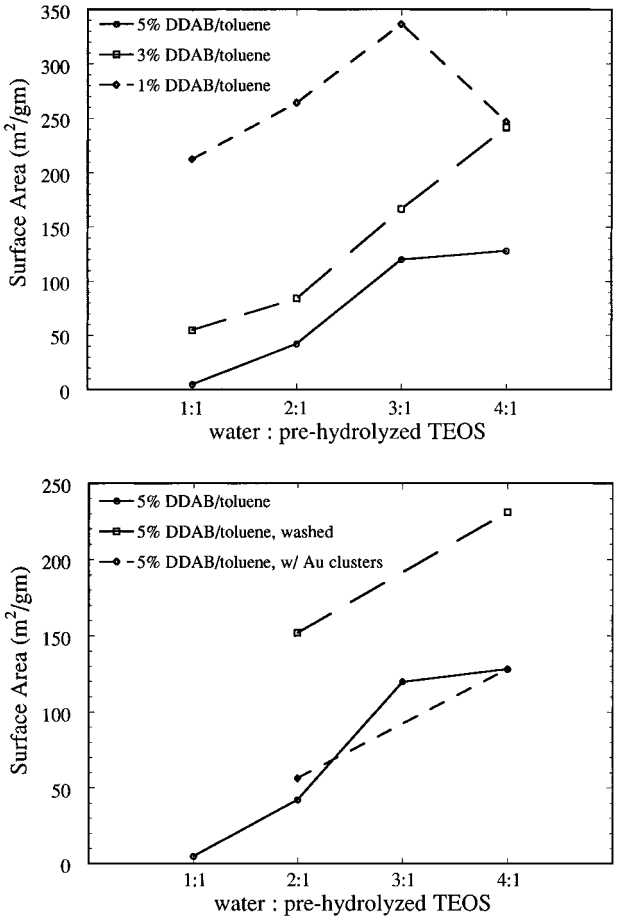

Figure 7. (a, top) BET surface areas of prehydrolyzed TEOS aerogels as a function of the H_2O:Si ratio and surfactant concentration. Au salt or clusters are not present. The trends established for TEOS materials are repeated. Surface areas generally increase with the reaction stoichiometry and decreasing surfactant concentration. Prehydrolyzed TEOS xerogel surface areas are smaller, but follow similar trends. (b, bottom) BET surface areas of prehydrolyzed TEOS aerogels as a function of hexanol washing and cluster presence. The trends established for TEOS materials are repeated. Surface areas increase when surfactant is washed from the pores. The presence of Au salt or clusters has no effect of gel surface areas.

size and the material exchange rate depend on experimental parameters such as the surfactant/solvent system, the addition of water which swells the inverse micelles, and the salt-to-surfactant ratio. Particle size control is often complicated but feasible. Our work with the TEOS, DDAB, and toluene system establishes three results: (1) the reduction reaction in TEOS inverse micelle solutions and in gelled samples produces particles roughly 2 times larger than particles formed in only DDAB/toluene mixtures,[67] (2) the gelation has little effect on the final particle size as determined by the plasmon resonance but does influence the initial growth rate, and (3) the particle size is not dependent on the gel precursor type, the reaction stoichiometry, or the drying method.

The effect of TEOS on the inverse micelle structure and the cluster growth and stabilization processes is the likely cause for the increased particle size in the mixtures studied here compared to particles synthesized in traditional DDAB/toluene mixtures. Cluster nucleation and growth is sustained within the inverse micelles. A change in micelle structure and the growth and stabilization process is inferred from the effects of TEOS on the surfactant aggregation phenomena as detected by SAXS. With the addition of the base and water solution, hydrolysis and condensation of the TEOS starts. The presence of water and the further production of water and alcohol in the reactions further destabilize the inverse micelle structure and causes the clusters to grow at a faster rate as evidenced by the UV−visible absorption spectra. However, the final particle size is unchanged in gelled systems compared to ungelled systems. Apparently, an upper bound in the stabilization process is reached.

Some of the variables adjusted in this study to control material properties include the gel precursor type, the water-to-gel precursor reaction stoichiometry, and the drying process (xerogels vs aerogels). The precursor type and drying process would have no direct effect on particle size control, and none was observed. More typical methods to control particle size include the surfactant/solvent system, the metal salt-to-surfactant ratio, and water content. Different surfactant/solvent systems were explored in this study (poly(oxyethylene)-(6) nonyl phenyl in cyclohexane and tetraethyleneglycol mono-*n*-dodecyl ether in octane), but results were less fruitful. Silica particles resulted, or phase separation occurred with only the water-rich phase gelling.[68] Salt-to-surfactant ratios were not varied in this study. We attempted to control particle size through the use of

water content. No particle size control is apparent in this effort most likely due to the destabilization of the inverse micelle structure in the presence of TEOS and the hydrolysis and condensation byproducts. However, the principles of particle size control remain in this methodology and further effort is required.

Despite the lack of particle size control, the role of the surfactant is clear. The inverse micelles act to solubilize the metal salt, stabilize the clusters against growth, and solubilize the TBAOH/H_2O mixture during gelation. If surfactant is not used, little $AuCl_3$ is solubilized in TEOS, toluene mixtures ($<<0.001$ M). Reduction with $LiBH_4$ results in large particles that are stable for only a few hours. Finally, introduction of the TBAOH/H_2O mixture results in immediate precipitation of the clusters, phase separation of a water-rich and an oil-rich phase, and no gelation.

In traditional sol−gel chemistry, the relative rates of hydrolysis and condensation as effected by sol−gel processing parameters such as acid- vs base-catalyzed reactions and the H_2O:Si ratio control the final gel properties.[69,70] In general, hydrolysis dominates under acid-catalyzed, low H_2O:Si ratio conditions and weakly branched, polymeric sols and gels are produced. Condensation dominates under base-catalyzed, high H_2O:Si ratio conditions to produce highly condensed particulate sols and gels. As condensation rates increase, gelation time and gel surface areas generally decrease.

For gels prepared with TEOS in inverse micelle solutions as the H_2O:Si ratio increases, gel times and surface areas increase in direct contradiction to the above stated conventional wisdom. We propose that the mechanism of gelation in the cluster solutions depends on the relative solubilities of the reactants in various "areas" of the microheterogeneous solutions. TEOS is soluble in toluene, and DDAB is soluble in TEOS. Thus, TEOS most likely exists within the inverse micelle and throughout the solution. Decreased aggregation of DDAB in toluene with the introduction of TEOS as detected by SAXS supports this hypothesis. Added water is soluble only within the inverse micelle. Thus, it is likely that gelation occurs mostly at the surfactant interface. Two important results stem from this hypothesis. First, the effective H_2O:Si ratio is much higher than expected from the set H_2O:Si recipe resulting in high condensation rates. As a result, gels are formed in this study even at low H_2O:Si recipes, and surface areas of TEOS gels are low. Second, with increasing H_2O:Si ratio, the H_2O:DDAB ratio increases. Increasing the H_2O:DDAB leads to larger, more polydisperse inverse micelles and a subsequent decrease in the surface area of reaction. Increasing the H_2O:Si recipe actually leads to a decrease in the effective H_2O:Si ratio, and thus, lower condensation rates and the observed higher surface areas and faster gel times. While the proposed gelation mechanism explains the existing data, it is clearly not universally applicable. Monoliths are not formed in other inverse micelles systems, and the use of other structured surfactant phases produce periodic silica phases.[71−73]

Gel surface areas increase with decreasing surfactant concentration. This result is consistent with our proposed mechanism. As surfactant concentration decreases, the H_2O:DDAB ratio increases resulting in a decrease in the surface area of the reaction. Decreasing surfactant concentration leads to lower effective H_2O:Si ratios, lower condensation rates, and the observed higher surface areas. It is apparent from the increase in the gel surface area after the surfactant is washed away that surfactant also blocks the available gel surface.

Gelation times are faster and surface areas are higher when the prehydrolyzed form of TEOS is used. These results indicate that the condensation rates for the prehydrolyzed TEOS precursor reactions are slower than for the TEOS precursor reactions. Steric effects are most likely responsible for the slower condensation rates with the bulkier precursor.

Conclusions

We have encapsulated nanometer-sized Au particles in the micropores of xerogels and aerogels. The synthesis is a sequential reduction of a gold salt and sol−gel processing in an inverse micelle solution. The inverse micelle solution is used to solubilize the metal salt and provide a microreactor for the nucleation, growth, and stabilization of the nanometer-sized clusters. Hydrolysis and condensation of an added siloxane precursor produces a wet gel embedding the particles. The presence of gel precursors destabilizes the inverse micelle structure resulting in larger particle sizes compared to typical inverse micelle synthesis techniques. Particle size control is complicated by the gel precursor effect on inverse micelle structure and the production of water and alcohol in the hydrolysis and condensation reactions. Finally, a unique gelation technique is outlined in these microheterogeneous solutions. Gelation occurs across the surfactant interface increasing the effective H_2O:Si ratio. Gelation occurs even at low H_2O:Si ratios, and condensation rates are high. Sol−gel parameters such as the H_2O:Si ratio and the surfactant concentration have unique and sometimes not intuitive effects on the hydrolysis and condensation rates and the resulting material properties.

Acknowledgment. The authors thank Thomas Headley of the Electron Microscopy/Metallography Department at Sandia for the TEMs, Edward M. Russick of the Organic Materials Processing Department at Sandia for the supercritical extractions, Duen Wu Hua and Thomas P. Rieker of the University of New Mexico for the SAXS, and Steven K. Showalter of the Solar Thermal Technology Department at Sandia. This work is supported by the U.S. Department of Energy under contract DE-AC04-94AL85000. Sandia is a multiprogram laboratory operated by Sandia Corp., a Lockheed Martin Co., for the United States Department of Energy.

CM9604625

(68) As mentioned in the Introduction, other inverse micelle solutions have been used in gelation reactions, but surfactant or alcohol concentrations are high. These recipes are unsuitable in our cluster synthesis. Cluster synthesis was not attempted in the other studies.

(69) Brinker, C. J.; Scherer, G. W. *Sol−Gel Science—The Physics and Chemistry of Sol−Gel Processing*; Academic Press: San Diego, 1990.

(70) Ward, D. A.; Ko, E. I. *Ind. Eng. Chem. Res.* **1995**, *34*, 421.

(71) Kresge, C. T.; Leonowicz, M. E.; Roth, W. J.; Vartuli, J. C.; Beck, J. S. *Nature* **1992**, *359*, 710.

(72) Monnier, A.; Schuth, F.; Huo, Q.; Kumar, D.; Margolese, D.; Maxwell, R. S.; Stucky, G. D.; Krishnamurthy, M.; Petroff, P.; Firouzi, A.; Janicke, M.; Chmelka, B. F. *Science* **1993**, *261*, 1299.

(73) Huo, Q.; Margolese, D. I.; Ciesla, U.; Feng, P.; Gier, T. E.; Sieger, P.; Leon, R.; Petroff, P. M.; Schuth, F.; Stucky, G. D. *Nature* **1994**, *368*, 317.